Frequency self-doubling optical parametric amplification: noncollinear red–green–blue light-source generation based on a hexagonally poled lithium tantalate

P. Xu, Z. D. Xie, H. Y. Leng, J. S. Zhao, J. F. Wang, X. Q. Yu, Y. Q. Qin, and S. N. Zhu*

National Laboratory of Solid State Microstructures, Nanjing University, Nanjing, 210093, China
*Corresponding author: zhusun@nju.edu.cn

Simultaneous generation of noncollinear red, green, and blue light from a single hexagonally poled lithium tantalate is reported. It results from the frequency self-doubling optical parametric amplification process, a process of second-order harmonic generation cascaded optical parametric amplification in a single-pass setup. The temperature and spectrum detuning characters of each cascaded quasi-phase-matching process are studied. This unique red–green–blue light source has potential applications in laser display and other laser industries. © 2008 Optical Society of America

OCIS codes: 190.4410, 140.7300, 190.4400.

The cascaded nonlinear process has attracted great interest in recent years, since it can extend light wavelength to shorter or longer extents [1–20]. It usually requires more than one second-order nonlinear crystal or relies on coincidental crossing of several phase-matching curves inside one nonlinear crystal in which birefringence phase matching (BPM) is utilized [1–7]. However, for this type of cascaded optical parametric process, the $\chi^{(2)}$-modulated nonlinear crystal, also called quasi-phase-matching (QPM) material, should have more advantages. People can modulate $\chi^{(2)}$ to realize intense coupling between arbitrary parametric processes inside one single crystal. Pioneer work including second-order harmonic generation (SHG) or sum frequency generation (SFG) cascaded optical parametric oscillation (OPO), etc., have been accomplished through QPM inside a one-dimensional (1D) periodically, quasi-periodically, or aperiodically poled crystal [8–20]. Some high-order harmonic generations even in a two-dimensional (2D) QPM crystal are achieved [21,22].

In this Letter we report on the experimental realization of self-doubling optical parametric amplification (OPA) process, a process of the signal or the idler doubling cascaded OPA inside a hexagonally poled lithium tantalate (HexPLT) crystal. The cascaded SHG of the signal or the idler together with the OPA process both reach a high efficiency in a single-pass setup. The simultaneous happening SHGs of the signal and the idler together with the residual pump light generate a set of red–green–blue (RGB) primary colors in vision. The special tuning characters on temperature, wavelength, angle, etc. of this HexPLT imply that it is a novel candidate for a high-gain RGB light source and other multiple-wavelengths generators.

In the experiment the HexPLT sample is fabricated by the electric field poling technique [23,24]. Figure 1(a) shows its domain structure after being slightly etched in acids. The near circularly inverted domains

(with radius r) distribute hexagonally in the $+\chi^{(2)}$ background with structure parameter $a = 9.05\ \mu$m. We define the reversal parameter $r/a = 28\%$, and the corresponding duty cycle $f = 2\pi r^2/\sqrt{3}a^2$ is then 28%. No domain merging is found across the whole sample dimensions of 15 mm $(x) \times 5$ mm (y) with a thickness of 0.5 mm. For each reciprocal lattice vector (RLV) there are six equivalent ones as shown in Fig. 1(b) owing to the sixfold degeneration of this structure.

The general phase-matching condition for nonlinear interaction in the QPM material is $\vec{k}_3 - \vec{k}_1 - \vec{k}_2 - \vec{G}_{m,n} = 0$ [25,26], where $\vec{G}_{m,n} = (4\pi/\sqrt{3}a) \times (\sqrt{m^2 + n^2 + mn})$ is the RLV of the HexPLT with lattice parameter a and the subscripts m and n are integers, representing the order of RLV; $\vec{k}_1$, $\vec{k}_2$, and $\vec{k}_3$ represent the interacted three waves. The pump beam is a 10 Hz 532 nm laser with a pulse width of 3.5 ns and a linewidth of 0.1 nm. We use an $f = 150$ mm lens to focus this $\hat{z}$-polarized pump beam into the HexPLT crystal, getting the beam waist to be around 120 μm.

When the pump beam incidence is along the direction of $\vec{G}_{0,1}$ ($\hat{x}$ axis) and we tune the crystal temperature during 20°C–200°C, a QPM collinear paramet-
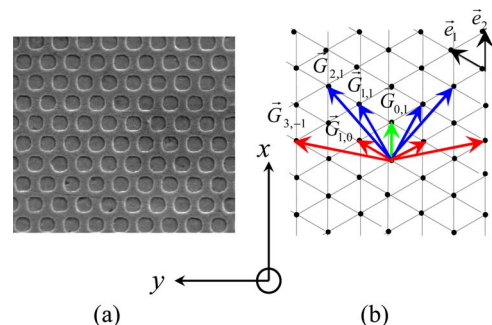

Fig. 1. (Color online) (a) Micrograph of the HexPLT and (b) its reciprocal space.

© 2008 Optical Society of America

ric downconversion process happens and the momentum conservation is ensured by $\vec{k}_p - \vec{k}_s - \vec{k}_i - \vec{G}_{0,1} = 0$. The measured wavelength of the signal and the idler varying on temperature is shown in Fig. 2, which consists well with the theoretical calculation. A wide spectrum about 500 nm is covered when the temperature varies from 20°C to 200°C.

Two incidental SHG processes occur simultaneously when the temperature is set around 188°C. The QPM condition for the signal and the idler doublings are $\vec{k}_{ui} - 2\vec{k}_i - \vec{G}_{1,0} = 0$ and $\vec{k}_{us} - 2\vec{k}_s - \vec{G}_{2,1} = 0$, respectively. Coupling these two noncollinear SHG processes with the OPA process is called dual-frequency self-doubling OPA. At 188°C, the signal and the idler are 868.3 and 1373.6 nm and both are collinear with the pump beam. As shown in the insets of Fig. 2, the harmonics of the signal and the idler both shape a pair of spots on the screen behind the crystal. The upper pair is the harmonics of the idler with the central frequency of 686.8 nm, while the lower pair is the harmonics of the signal with the central frequency of 434.2 nm. The mirror symmetry of these two pair spots about the pump beam is due to the mirror symmetry of involved RLVs $\vec{G}_{2,1}$ and $\vec{G}_{1,0}$. The energy of two red spots and two blue spots are 11 and 5.2 μJ, respectively, under the pump energy of 1.17 mJ. Adding the remaining pump at 532 nm, we get a set of three primary colors. According to the Commission Internationale de l'Eclairage (CIE) chromaticity diagram [27], this set of RGB light can cover most of the area in the CIE chromaticity diagram, which can be used uniquely in laser displays, laser TV, etc.

Actually the temperature of 188°C is deviated from the maximum output temperature for both the red and the blue generation. When lowering the temperature down to 179.6°C, the idler doubling process approaches its maximum efficiency, and the external angle is getting larger toward 5.5° as shown in Fig. 3. The fitted temperature FWHM is around 16°C, which is rather big when compared with 1D periodically poled lithium tantalate (PPLT). It mostly results from the noncollinear phase-matching character in this HexPLT, which has been verified by some
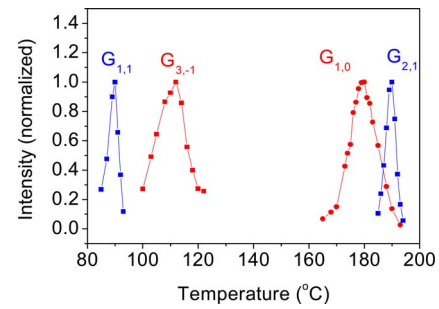
Fig. 3. (Color online) Intensity versus temperature for each frequency self-doubling process.

earlier work [21]. When the temperature is at 179.6°C, the efficiency of the idler into its harmonics reaching its maximum is about 30% while the efficiency of the idler over the pump is about 10.8% under a pump energy of 1.17 mJ.

The pair of blue spots, i.e., the frequency doubling of the signal, approaches its maximum efficiency at 189.5°C while the bandwidth is 6°C. It can be seem from Fig. 3 that owing to the wide temperature bandwidth of the signal and the idler doubling processes, it is not hard to reach simultaneously red and blue beams within some range of temperature.

Another dual-frequency self-doubling OPA process is observed around 100°C in this HexPLT. The signal and idler wavelength are 932.33 and 1240.68 nm, hence the corresponding harmonic waves are at 466.17 and 620.34 nm. Therefore we can get another set of three elementary colors when taking the 532 nm pump into account. Momentum conservations for the idler and signal doubling are $\vec{k}_{ui} - 2\vec{k}_i - \vec{G}_{3,-1} = 0$ and $\vec{k}_{us} - 2\vec{k}_s - \vec{G}_{1,1} = 0$, respectively. The idler and the signal doubling shape another pair of red spots and blue spots with mirror symmetry on the screen behind the crystal. At 110.3°C the idler doubling reaches its maximum and the temperature detuning bandwidth is about 16.6°C, while the signal doubling reaches it maximum at 89.4°C and the bandwidth is about 5.3°C.

In Table 1, we list the detailed detuning characters of four frequency self-doubling processes when the temperature changes from room temperature to 200°C. For each signal or idler doubling process, the linewidth $\Delta\lambda$, the external angle α_{ext}, and the relative intensity of the harmonics (λ_d) are listed. We investigate the intensities of four self-doubling processes under the condition of low pump power, which ensures the nondepleted pumping approximation. The experimental and the theoretical results are shown in the last two columns and consist well. The idler doubling process happening around the 179.6°C participant by $\vec{G}_{0,1}$ has the maximum output intensity.

It is worth noting here that when we choose the hexagonal structure only one freedom, i.e., the lattice parameter a, can be adjusted to meet the phase-matching requirements. So it is natural that the red and blue are generated not exactly simultaneously. In principle for exact simultaneous phase-matching of the signal and idler doubling, additional structure freedoms should be introduced. Other structures,
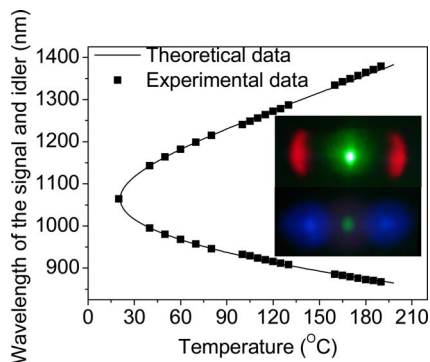

Fig. 2. (Color online) Temperature-dependent curve for the OPA process. The insets are the photographs of the signal harmonics participant by $\vec{G}_{1,1}$ or $\vec{G}_{2,1}$ and the idler harmonics participant by $\vec{G}_{3,-1}$ or $\vec{G}_{1,0}$ when filtering out most of the pump.

Table 1. Detailed Detuning Characters of Four Frequency Self-Doubling Processes[a]

$T\ (\Delta T)$ (°C)	$\lambda_s\ (\Delta\lambda_s)$ (nm)	$\lambda_i\ (\Delta\lambda_i)$ (nm)	$\lambda_d\ (\Delta\lambda_d)$ (nm)	α_{ext} (°)	$G_{m,n}$	$f_{m,n}$	I_d(exp.) (a.u.)	I_d(theo.) (a.u.)
89.4(5.3)	937.5(6.0)	1230(12)	468.7(0.5)	3	$\vec{G}_{1,1}$	0.04	1	1
110.3(16.6)	920.8(5.5)	1260(10)	630(5.0)	12	$\vec{G}_{3,-1}$	0.07	3.3	2.3
179.6(15.9)	873(4.0)	1362(7.3)	681.2(3.3)	5.5	$\vec{G}_{1,0}$	0.32	40	40
189.5(6.0)	867(2.6)	1379(7.7)	433(1)	5	$\vec{G}_{2,1}$	0.07	8	3

[a]The theoretical calculation including the Fourier coefficients f_{mn} and the intensity of the harmonics I_d(theo.) are based on the real duty cycle about 28% of the HexPLT.

such as a 2D structure with a parallelogram unit or a 2D fractal structure, can be adopted. In addition, to further enhance the red–blue intensity from this HexPLT, we can put it into an optical cavity that will give the signal or idler high feedback.

In conclusion, we designed and observed two sets of dual-frequency self-doubling processes in an HexPLT crystal, two sets of signal and idler SHGs cascaded an OPA process. QPM ensures such multiple processes happening inside a single crystal and also enables a high-gain output in this single-pass setup. The generation of the red–blue light together with the remaining green pump from the HexPLT is a new method for noncollinear three primary colors output without any optical separation elements. This unique light source has potential applications in laser display, multicolor laser generation, integrated optics etc.

References

1. R. A. Andrews, H. Rabin, and C. L. Tang, Phys. Rev. Lett. **25**, 605 (1970).
2. J. M. Yarborough and E. O. Ammann, Appl. Phys. Lett. **18**, 145 (1971).
3. V. Petrov and F. Noack, Opt. Lett. **20**, 2171 (1995).
4. T. Kartaloğlu, K. G. Köprülü, and O. Aytür, Opt. Lett. **22**, 280 (1997).
5. K. G. Köprülü, T. Kartaloğlu, Y. Dikmelik, and O. Aytür, J. Opt. Soc. Am. B **16**, 1546 (1999).
6. E. C. Cheung, K. Koch, and G. T. Moore, Opt. Lett. **19**, 1967 (1994).
7. R. J. Ellingson and C. L. Tang, Opt. Lett. **18**, 438 (1993).
8. G. T. Moore, K. Koch, M. E. Dearborn, and M. Vaidyanathan, IEEE J. Quantum Electron. **34**, 803 (1998).
9. O. Pfister, J. S. Wells, L. Hollberg, L. Zink, D. A. Van Baak, M. D. Levenson, and W. R. Bosenberg, Opt. Lett. **22**, 1211 (1997).
10. C. McGowan, D. T. Reid, Z. E. Penman, M. Ebrahimzadeh, W. Sibbett, and D. H. Jundt, J. Opt. Soc. Am. B **15**, 694 (1998).
11. G. Z. Luo, S. N. Zhu, J. L. He, Y. Y. Zhu, H. T. Wang, Z. W. Liu, C. Zhang, and N. B. Ming, Appl. Phys. Lett. **78**, 3006 (2001).
12. X. P. Zhang, J. Hebling, J. Kuhl, W. W. Rühle, and H. Giessen, Opt. Lett. **26**, 2005 (2001).
13. W. R. Bosenberg, J. I. Alexander, L. E. Myers, and R. W. Wallace, Opt. Lett. **23**, 207 (1998).
14. S. N. Zhu, Y. Y. Zhu, and N. B. Ming, Science **278**, 843 (1997).
15. Y. B. Chen, C. Zhang, Y. Y. Zhu, S. N. Zhu, H. T. Wang, and N. B. Ming, Appl. Phys. Lett. **78**, 577 (2001).
16. K. F. Kashi, A. Arie, P. Urenski, and G. Rosenman, Phys. Rev. Lett. **88**, 023903 (2002).
17. Y. Zhang and B. Y. Gu, Opt. Commun. **192**, 417 (2001).
18. M. M. Fejer, G. A. Magel, D. H. Jundt, and R. L. Byer, IEEE J. Quantum Electron. **28**, 2631 (1992).
19. Z. D. Gao, S. Y. Tu, S. N. Zhu, and A. H. Kung, Appl. Phys. Lett. **89**, 181101 (2006).
20. X. P. Hu, G. Zhao, Z. Yan, X. Wang, Z. D. Gao, H. Liu, J. L. He, and S. N. Zhu, Opt. Lett. **33**, 408 (2008).
21. N. G. R. Broderick, R. T. Bratfalean, T. M. Monro, D. J. Richardson, and C. M. de Sterke, J. Opt. Soc. Am. B **19**, 2263 (2002).
22. N. Fujioka, S. Ashihara, H. Ono, T. Shimura, and K. Kuroda, J. Opt. Soc. Am. B **24**, 2394 (2007).
23. S. N. Zhu, Y. Y. Zhu, Z. Y. Zhang, H. Shu, H. F. Wang, J. F. Hong, C. Z. Ge, and N. B. Ming, J. Appl. Phys. **77**, 5481 (1995).
24. P. Xu, S. H. Ji, S. N. Zhu, X. Q. Yu, J. Sun, H. T. Wang, J. L. He, Y. Y. Zhu, and N. B. Ming, Phys. Rev. Lett. **93**, 133904 (2004).
25. V. Berger, Phys. Rev. Lett. **81**, 4136 (1998).
26. N. G. R. Broderick, H. L. Offerhaus, G. W. Ross, D. J. Richardson, and D. C. Hanna, Phys. Rev. Lett. **84**, 4345 (2000).
27. http://www.nd.edu/~sboker/ColorVision2/ CIEColorSpace2.gif.